NASA TECHNICAL NOTE

NASA TN D-2571

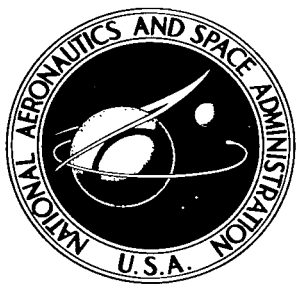

SOME TRANSIENT ELECTRICAL CHARACTERISTICS OF THE EXHAUST OF A SELF-CROWBARRED COAXIAL PLASMA GUN

by Charles J. Michels

Lewis Research Center

Cleveland, Ohio

NATIONAL AERONAUTICS AND SPACE ADMINISTRATION • WASHINGTON, D. C. • JANUARY 1965

SOME TRANSIENT ELECTRICAL CHARACTERISTICS OF THE EXHAUST OF A SELF-CROWBARRED COAXIAL PLASMA GUN

By Charles J. Michels

Lewis Research Center
Cleveland, Ohio

NATIONAL AERONAUTICS AND SPACE ADMINISTRATION

For sale by the Office of Technical Services, Department of Commerce,
Washington, D.C. 20230 -- Price $1.00

SOME TRANSIENT ELECTRICAL CHARACTERISTICS OF THE EXHAUST OF A SELF-CROWBARRED COAXIAL PLASMA GUN*

by Charles J. Michels

Lewis Research Center

SUMMARY

An experimental investigation of the discharge from a self-crowbarred coaxial plasma gun was performed by using Rogovsky loops, framing and streak cameras, and magnetic-field probes. The discharge appears first as a weak-intensity diffuse plasma puff, whose velocity, as determined from streak-camera photographs, is the same as the velocity of the current front, as determined by magnetic probes in the gun annulus. Its location coincides with the extrapolated location of the current front.

A short time later, an intense well-collimated elongating luminous core of plasma appears from the tip of the center electrode. The velocity of this core front is slightly less (and diminishing with time) than the current-front velocity. Rogovsky loop measurements indicate that this core is part of a closed current path between the gun electrodes and is current-carrying at a point well downstream of the muzzle.

INTRODUCTION

In examining the possible application of a coaxial plasma gun for space propulsion, a detailed knowledge of the gross nature of the exhaust characteristics must be provided. This knowledge is needed to determine thrust and also the effects of the exhaust on exhaust instrumentation. An experimental approach to the understanding of the structure of the exhaust, the electrical currents flowing in the plume, and the velocity of fronts in portions of the plume is described herein.

The gun used in this work is similar to that described by Marshall and others (refs. 1 to 9) rather than an annular shock-tube device (refs. 10 to 13)

---

*This report is an expanded version of the paper presented at the American Physical Society Summer Meeting in the East, June 5, 1963, Buffalo, N.Y.

or guns having short center electrodes (refs. 14 to 16).

All of these devices generate a plasma sheet and accelerate the plasma sheet in the annulus between coaxial cylindrical electrodes. The action of the self-magnetic field created in the annulus by the current flow provides the accelerating force. This general statement is characteristic of all coaxial plasma guns.

A puff of propellant gas is introduced into the evacuated gun annulus, and the gas is ionized and accelerated by switching a capacitive energy storage system to the electrodes. The primary plasma sheet is formed in the annulus and moves along the barrel by the action of the magnetic-field pressure behind it. In Marshall's paper (ref. 1), after each half period of electrical current oscillation, a new plasma sheet was formed at the breech and moved along the gun barrel, somewhat behind and less energetic than the previous sheet. In the gun used in this experiment, which has been previously described by Michels and Ramins (ref. 2), the gas propellant is injected about midway along the barrel length, and as a result, the primary discharge is initiated at that location. As the primary sheet neared the nozzle, a secondary static discharge occurred internally at the breech. This is termed a "self-crowbar discharge" and is so named because the device itself creates this discharge internally and the discharge acts as an electrical switch (analogous to the "crowbar" switch used to prolong magnetic fields in confinement experiments for controlled thermonuclear research) that prevents the magnetic-field energy in the gun from returning to the capacitive energy storage system. Thus, the exhaust in this experiment is a single puff complicated by the action of the self-crowbar discharge.

The equivalent circuit of the bank and gun is schematically shown in figure 1 to aid in understanding the effect of the secondary discharge. The energy stored in the capacitor C_b, which has a small resistance R_b and inductance L_b, is switched to the load, the gun, by switch S_1. After the primary moving plasma sheet is formed, the electrical equivalent of the gun can be considered as a small resistance R_g and a time-varying inductance $L_g(t)$. At a later instant when most of the energy is in the magnetic field of the inductance and when the voltage across the gun electrodes changes polarity, a secondary static discharge develops in the gun at the breech, which can be considered in the equivalent circuit as the closing of the self-crowbar switch S_2. If the impedance of S_2 is low enough, its closing will prevent the stored inductive energy in the gun from returning to the capacitor. This inductively stored energy will decay monotonically thereafter with the field continuing to drive the moving plasma sheet.

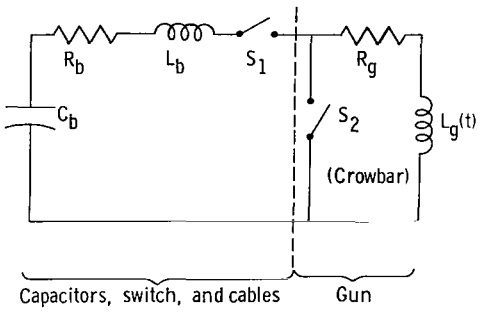

Figure 1. - Equivalent circuit of bank and gun.

The purpose of this experiment is to examine the nature of the current and front velocities of the exhaust plume for the self-crowbar type of operation of a coaxial plasma gun. It was suspected that the nature of the plume in this method of operation might be seriously different from the modes previously investigated. The structure of the plume can seriously affect the measurement

and interpretation of exhaust characteristics that are commonly used to evaluate the performance of the gun as a propulsion device.

Many authors have contributed to an understanding of gun exhaust characteristics. Representative of the diagnostic techniques employed are:

(1) Magnetic probes (refs. 1, 2, 3, 6, 10, 12, 17, 18, and 19)

(2) Calorimeters (refs. 1, 2, 4, 7, 17, 20, and 21)

(3) Streak and frame cameras (refs. 4, 5, 17, and 22)

(4) Time-of-flight technique (refs. 1, 2, 7, 11, 20, and 23)

(5) Ion energy analyzers (refs. 1, 7, 17, 20, 23, 24, and 25)

(6) Spectroscopic analyzers (refs. 4, 11, 19, and 21)

(7) Pendulums (refs. 1, 3, 4, and 21)

(8) Electric probes (refs. 3, 6, 18, 20, 24, and 26)

Each technique provides specific knowledge and is complementary to the problem of understanding exhaust characteristics. This experiment employed various Rogovsky loops (refs. 27 and 28) selectively placed in the exhaust to study gross currents in the plume structure. An image-converter camera was used for frame and streak photography to provide visualization of the structure of the luminous part of the plume related in time with loop and probe information. Magnetic probes in the gun annulus provided synchronization of exhaust measurements with related events while the plasma was in the gun confines.

After a description of the apparatus and procedure used, a discussion of the results of typical camera views and loop measurements follows. An exhaust model is described as a result of relating frame and streak views to loop measurements. A determination of typical velocities for the plume structure will also be discussed.

APPARATUS

Capacitor Bank

The capacitor bank used in this experiment is described in reference 2. It is an ignitron switched bank consisting of eleven identical sections in parallel each consisting of a 1.1-microfarad capacitor with its own ignitron switch. All sections are synchronously switched and connected through cabling to the coaxial plasma gun. Bank characteristics for this experiment are as follows:

Bank voltage (variable), kv	10 to 30
Bank resistance, ohms	3×10^{-3}
Bank inductance, mμh	10
Bank capacitance, μf	12.1
Shorted bank ringing frequency, kc	480
Switch jitter and repeatability, sec	of order of 10^{-8}

The mode of operation is such that the bank is switched from an external trigger signal.

Coaxial Plasma Gun

The gun used in this experiment has the following dimensions:

Overall length, cm	48
Inside diameter of outer electrode, cm	9.5
Outside diameter of inner electrode, cm	3.2
Gas port location from breech end (38 percent of gun length), cm	18.3
Length of insulator at breech, cm	9
Location of probe ports in outer electrode from breech end, cm	7.0, 18.5, 30.0, 41.5

The fast-acting gas valve used to inject a short-duration puff of gas into the electrode annulus was adjusted so that the puff duration is less than 100 microseconds. Hydrogen gas was allowed to expand in the gun annulus for 550 microseconds before the capacitor bank was switched to the gun electrodes. The gun electrodes were made of oxygen-free high-conductivity copper.

Rogovsky Loops

The gun fires into a 6-inch glass pipe cross, which is used as a measurement and observation section. Inside the measurement section shown in figure 2 is a movable survey Rogovsky loop oriented normal to the gun axis and having an active loop diameter about the size of the gun center electrode diameter. This loop can be moved to various radial positions in the exhaust, and it is used to monitor the time derivative of current threading the loop. References 27 and 28 describe the pertinent equations and design details of Rogovsky loops. The output of the loop

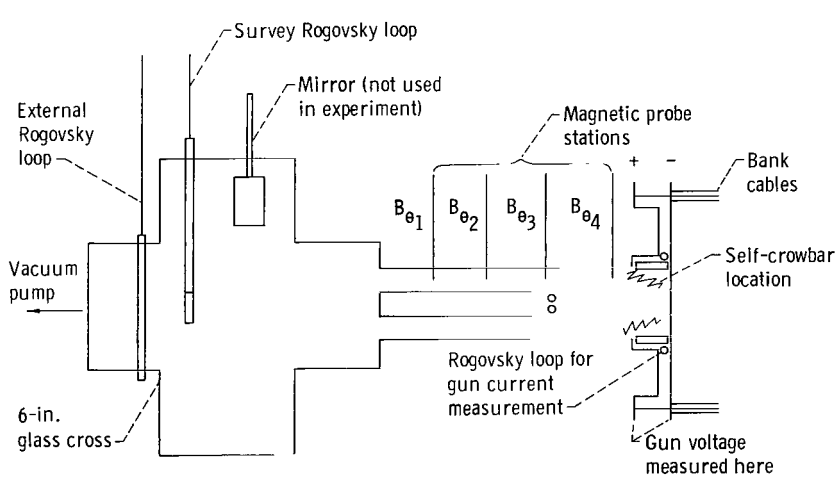

Figure 2. - Top view of gun and measurement section.

used was transmitted by coaxial cable to a screen room. The signal cable was terminated, and the signal passively integrated. The integrator time constant was 10 microseconds. The integrated signal is proportional to current threading the loop, and this signal against time was recorded on an oscilloscope. The loop, the cable, and the integrator were calibrated as a unit by threading the loop with a wire carrying a known transient current having equivalent dynamics. The known current was determined by two independent methods: (1) it was measured by a secondary standard current transformer and (2) it was calculated from the transient circuit equations of the calibration circuit.

Figure 2 also shows another Rogovsky loop (labeled external Rogovsky loop) encircling the glass duct on the outside. This loop has increased sensitivity and its dynamic response, though slower than the survey loop, is still sufficient for the experimental conditions. This loop signal is transmitted, terminated, and integrated in the same manner as the survey loop. Calibration is also accomplished in the same fashion as described earlier. Tests of both loops showed that negligible signals resulted from electrostatic pickup or unwanted field pickup.

Image-Converter Camera

An image-converter camera was used to view exhaust phenomena in the center of the glass measurement section. A viewing window on one end of the cross was provided for this camera. The image-converter camera was used as a framing camera for these views. Another viewing position for the camera was also used. This view was taken of the exhaust in the glass duct just as it leaves the gun muzzle. The camera was used in this position for either frame or streak views. The streak views were obtained by masking off all of the glass duct except for a 10-centimeter-long 2-millimeter-wide viewing slit on the glass duct alined with the center of the duct and parallel with the gun axis. The image-converter camera in framing operation was set for a 10-nanosecond exposure time per frame and for selectable delays between the three frame views that it sequentially records.

Since the gun phenomena are fully repeatable from shot to shot (after 10 conditioning shots) the first frame view is exposed on command from an external trigger signal that can be delayed precisely through delay electronics to view a phenomenon at a desired time synchronized with gun events. The other two frame views are delayed as chosen with respect to the first frame. When the image converter camera is used in the streak mode, the streak starts on command from an external trigger related to a synchronized gun event. The streak camera sweep duration in these tests is 2 microseconds.

Magnetic-Field Probes

Azimuthal magnetic-field probes are inserted (at known axial separations) in the gun annulus. The last of such probes is located near the gun muzzle. This probe detects the passage of the moving current sheet while it is inside the gun confines by detecting the sharp increase in magnetic field immediately behind the sheet. This probe is used to time reference exhaust phenomena with

gun sheet position and velocity. Other azimuthal probe locations are noted on page 4. Time of flight of the magnetic front between two adjacent stations determines the magnetic-front velocity.

The magnetic probes are 10-turn coils, solenoidally wound about a 0.050-inch-diameter coil form and encased in a 96-percent silica glass protector tube. The signals are transmitted, terminated, and integrated in the same fashion as the Rogovsky loop signals described earlier. The probes are calibrated by immersion in a known transient magnetic field with dynamics similar to those of the experiment.

Miscellaneous Instrumentation

Transient measurements of gun voltage and gun current were also recorded for the data described but were not used. This information was used to aid in determining the shot to shot repeatability, and also yielded some timing information.

The mirror shown in the glass-cross measurement section in figure 2 was not used in this experiment but is depicted there to orient the reader, since some of the frame views show the mirror in stored position.

PROCEDURE

The mass of propellant per shot (45 μg of hydrogen) was calibrated just prior to the series of shots. It was chosen to be near optimum to produce maximum energy in the exhaust for this bank charge, gun configuration, and gas (ref. 2). The time delay between propellant injection and application of bank voltage to the gun electrodes was determined from prior testing. It was found to be optimum at 550 microseconds for maximum energy in the exhaust.

Oscilloscope sweeps were synchronized, and sweep linearity was checked just prior to the shots. A gain and frequency response check of each oscilloscope was also performed.

The gun annulus and the measurement section were evacuated to the low 10^{-6} torr pressure range prior to each shot, and a 6-inch diffusion-pump system continually evacuated the measurement section and gun annulus. In order that the bank and gun perform repeatably, a series of 15 conditioning shots at 2-minute intervals was fired. This conditions the bank ignitrons to hold off voltage more reliably and switch with minimum jitter and in full synchronization. Conditioning shots also outgas and prepare the gun electrode surfaces for repeatable formation and acceleration of the discharge. After conditioning shots have been completed, data-gathering shots are performed as soon as possible.

For each shot the following sequence occurs:

(1) The bank is brought up to 15 kilovolts charge.

(2) The charging circuitry is disconnected.

(3) Each oscilloscope is reset for single sweep on command.

(4) The fast-acting gas valve is actuated to introduce the propellant. This actuation starts an electronic delay generator. After 550 microseconds the bank-trigger system is initiated.

(5) The "start" of the bank-trigger system also "starts" each scope sweep synchronously and "starts" a separate electronic time delay generator to operate the image-converter camera later at any preset time.

Data obtained from a set of identical shots as the exhaust reaches the measurement section consist of

(1) A radial Rogovsky loop survey of the axial current flowing in the exhaust time-related to (a) the magnetic-front arrival at the muzzle-most azimuthal magnetic-field probe and the (b) total current in the gun electrodes near the gun muzzle

(2) Time-related net current flowing in the exhaust and in the glass duct through use of the external Rogovsky loop

(3) Frame and streak views of the exhaust leaving the gun and frame views of the exhaust in the center of the measurement section

These were also time-related to the magnetic front in the annulus as it passes the magnetic-probe station nearest the muzzle.

The shot to shot repeatability of the exhaust and gun phenomena allowed viewing of different time regions of the exhaust under controlled conditions. A sufficient number of shots were taken under identical preset conditions so that, despite minor variations in mass per puff, one could select at least five shots that were truly identical with respect to all transient electrical characteristics. All data for these shots were synchronized to less than 0.1 microsecond. The exhaust structure and the currents in the self-crowbar mode of gun operation are shown for that operating point which, as described earlier, gives best energy efficiency and is also optimum for visual observation.

RESULTS AND DISCUSSION

Typical Traces

A typical set of data traces are presented in figure 3. These enable relating the magnetic probe and Rogovsky loop information to the transient voltage and current at the gun terminals.

The gun voltage V_g across the gun terminals is applied at time T_o. This occurs 550 microseconds after gas entry in the gun annulus. The corresponding gun current I_g is also shown. Since the self-crowbar discharge is downstream

of the gun-current sensor, the sensor notes the self-crowbar discharge occurrence in a not-too-evident fashion as a change in frequency. The self-crowbar discharge occurs at T_o plus 2.2 microseconds. Two magnetic probes (not described and whose data traces are not shown in fig. 3) provide a positive knowledge of the time that the self-crowbar discharge occurs. These probes, B_{θ_3} and B_{θ_4} (fig. 2, p. 4) used to sense the azimuthal magnetic field in the gun annulus, are located axially so that they are upstream of the initial moving discharge and downstream of the self-crowbar discharge. Traces from these probes show current in the moving discharge only and there is a definite change in waveshapes at the time when the self-crowbar discharge occurs. This can be determined to within 0.1 microsecond.

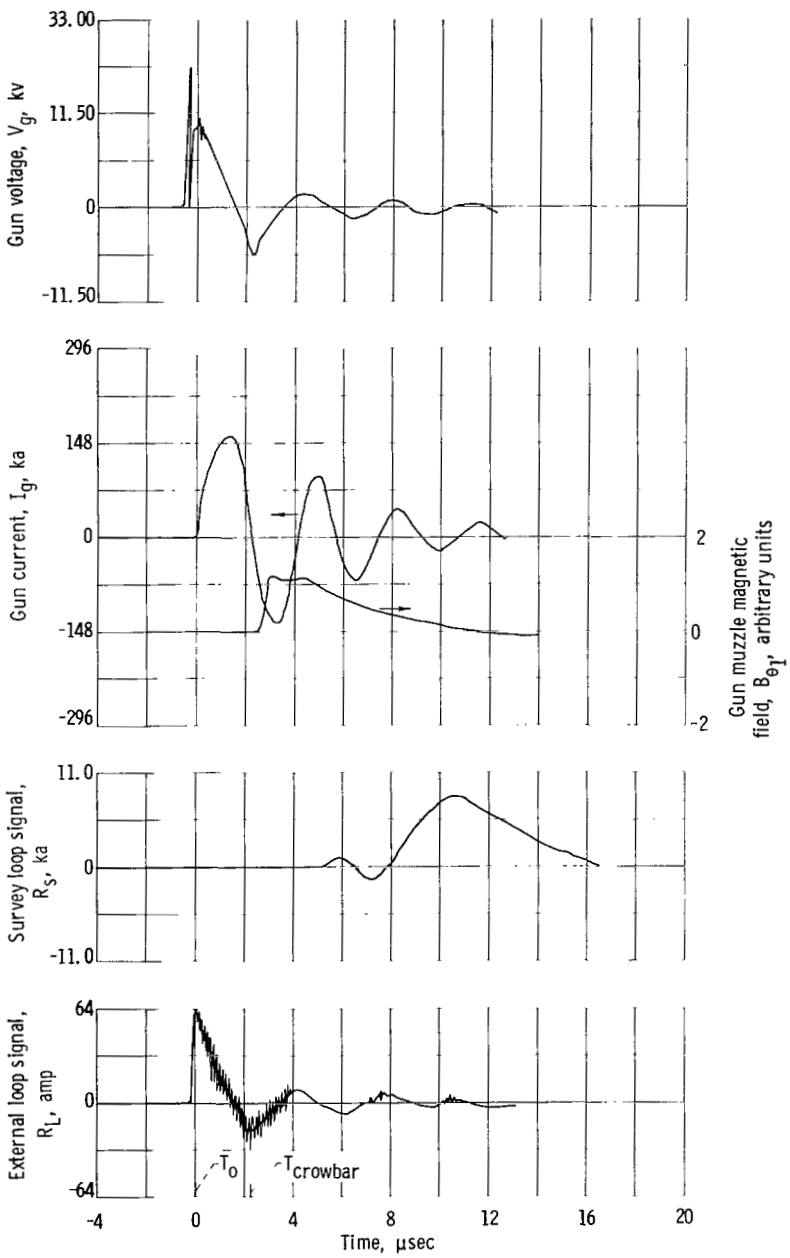

Figure 3. - Typical traces.

The azimuthal magnetic field in the gun annulus at the probe station nearest the muzzle B_{θ_1} shows magnetic-front arrival time as T_o plus 2.8 microseconds. The magnetic-field trace decays monotonically after T_o plus 4.5 microseconds. This is due to the action of the "crowbarred-in" field decaying as it expands against the moving current sheet. The droop in the trace obvious after about T_o plus 11 microseconds is caused by the integrator time constant being too small for the prolonged phenomenon being measured.

The integrated survey Rogovsky loop trace R_s shows no appreciable currents threading the loop until after T_o plus 6 microseconds. The loop is on the gun axis in the center of the measurement section located normal to the exhaust flow. After T_o plus 12 microseconds, the R_s trace shows a monotonic decaying signal. Any ob-

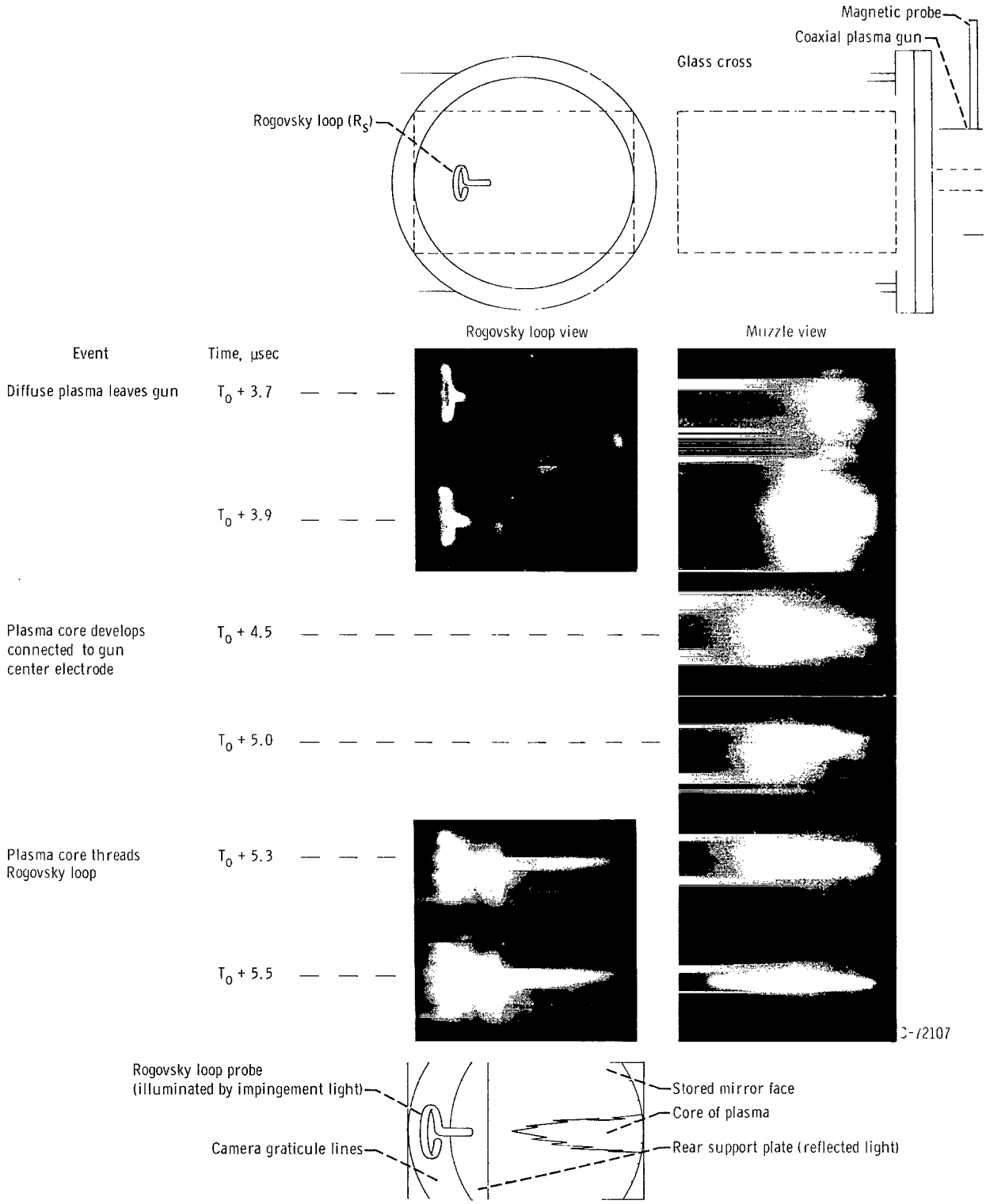

Figure 4. - Frame views of gun exhaust.

stacle in front of the loop R_S (such as an instrument probe), even though small compared with the loop diameter, perturbs the exhaust flow, and the exhaust current-carrying characteristics change. This perturbation was noted in a preliminary experiment not pertinent to this investigation and was noted visually as a deflection of the exhaust by the obstacle as well as by changes in the R_S trace. In this experiment, no obstacles were permitted upstream of the measurement location.

The integrated external Rogovsky loop trace R_L shows very small net currents in phase with and of the same shape as the gun voltage trace. These small leakage currents are always less than 1 percent of the main current and have no effect on the main findings of the experiment. The shapes, magnitudes, and time sequences of the traces shown in figure 3 occurred for all the B_{θ_1}, V_g, I_g, and R_L data traces recorded.

Frame Views of Gun Exhaust

Figure 4 shows sequential frame views of the exhaust in the measurement section. The figure shows the two viewing areas that were observed, the muzzle views and views of the exhaust entering the survey Rogovsky loop area of the measurement section.

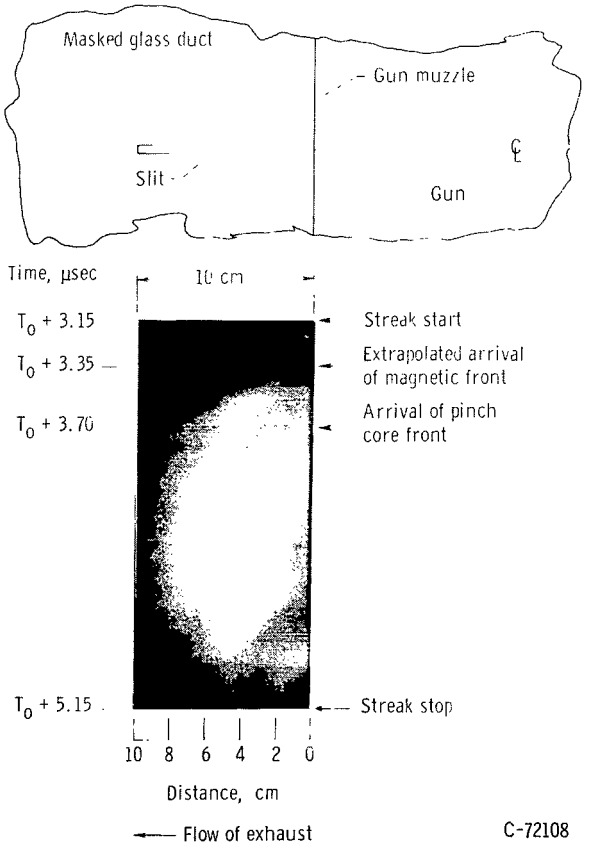

Figure 5. - Typical streak photograph of gun exhaust.

Muzzle views first show diffuse exhaust leaving the muzzle at the time expected for arrival of the magnetic front (predicted from front measurements of velocity and time of passage at the station nearest the muzzle). Later, after T_0 plus 4.0 microseconds, a core of plasma develops off the center electrode tip. It remains connected to the tip, with the core tip moving down the duct, and the core pinching down intensely.

The Rogovsky loop views, also shown in figure 4, indicate early impingement light from fast particles bombarding the survey loop much ahead of expected time arrival of the magnetic front. Reflected light from the gun cannot be this intense for the 10-nanosecond exposure time of the camera to record the effect. These fast particles are not luminous and are not associated with a significant axial current and thus cannot be examined in detail by using the diagnostic techniques of this experiment.

At time T_o plus 5.0 microseconds, the diffuse plasma moving with magnetic-front velocity has already passed, and the Rogovsky loop views show the pinch-core tip entering the field of view at the right (gun side). At T_o plus 5.5-microseconds, the tip is beginning to thread the survey Rogovsky loop. In the last two views the mirror edge can be seen in the background.

Streak Views of Gun Exhaust

A typical streak photograph of the exhaust taken through an axial slit on a masked-off portion of the measurement section at the gun muzzle is shown in figure 5. The sketch included orients the slit location with respect to the gun. The early fast particles are not visible in this photograph, but at about T_o plus 3.35 microseconds (also the extrapolated time of arrival of the magnetic front) a front enters the slit from the right. Its velocity (determined from the slope of the streak) is the same as the magnetic-front velocity measured by magnetic probes while the plasma is in the gun annulus. At T_o plus 3.7 microseconds, the pinch core develops on the axis and the core-tip front moves more slowly and with changing velocity. The slit is on the gun axis and the camera sees the intense pinch-core tip develop off the center electrode.

A comparison of the magnetic-front velocity in the gun with the diffuse plasma front velocity of the exhaust from streak photographs is shown in the table at the left. Agreement is very good for the four separate shots. The variation between these shots is probably due to mass per puff injection variations. The pinch-core tip-front velocity is changing and initially is about two-thirds of the diffuse velocity of the earlier diffuse front.

Run	Initial diffuse-front velocity of exhaust, cm/sec	Magnetic-front velocity inside gun, cm/sec
1	2.5×10^7	2.3×10^7
2	1.9	1.9
3	1.4	1.6
4	1.8	1.9

Rogovsky Loop Measurements

Radial loop survey. - Figure 6 shows the traces of typical radial survey Rogovsky loop signals. The survey Rogovsky loop trace is shown for three different but repeatable shots. Each trace is for a different radial position (fig. 7) of the loop in the measurement section.

No signals are noted until T_o plus 6 microseconds. Some plasma exhaust has already passed this station by this time, as noted by frame views described earlier. The time T_o plus 6 microseconds is coincident with the threading of a later developing collimated core of exhaust through the loop when the loop is on the gun axis. This, too, is confirmed by frame views of the core proceeding through the small loop.

The greatest amplitude of signals occurs when the survey loop is on the gun axis and shows 4.5-kiloampere currents in the exhaust threading the loop.

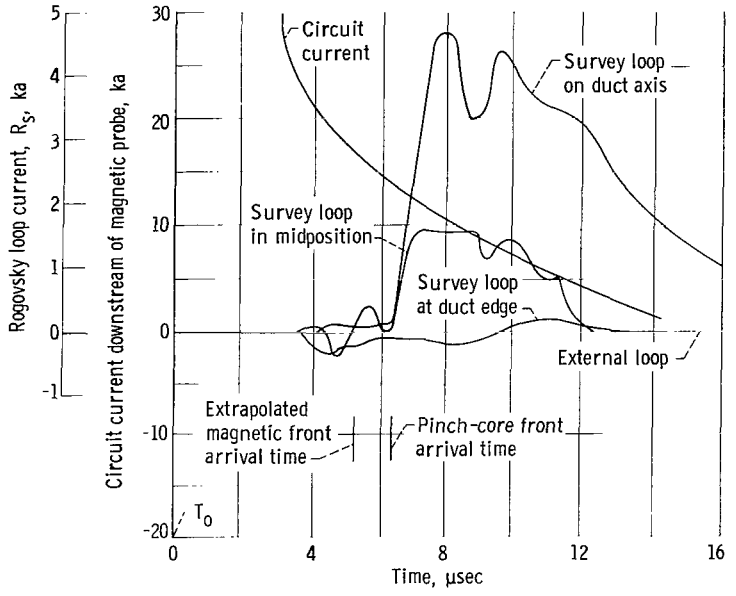

Figure 6. - Radial survey Rogovsky loop records.

These are unidirectional currents, consistent in polarity with center electrode currents and decaying monotonically. The 10-microsecond time constant of the loop signal integrator gives serious droop to the trace after a few microseconds but shows the qualitative trend.

Figure 6 shows peak currents of the order of 1 kiloampere for the case when the loop is in midposition. This signal occurs at the same time as the signal of the on-axis position probe. When the loop is in duct edge position, the signal shows a small current of opposite sign. This suggests that currents are returning along the duct edge plasma. A possible model of this later forming plasma structure is of cylindrically symmetrical shape with a central core of exhaust having axial currents proceeding down the core (as the core tip moves down the duct) and an outer cylinder of the plasma (near the duct wall) along which the core currents can return. This concept fits well with the frame views described earlier. An illustration of this model is shown in figure 8.

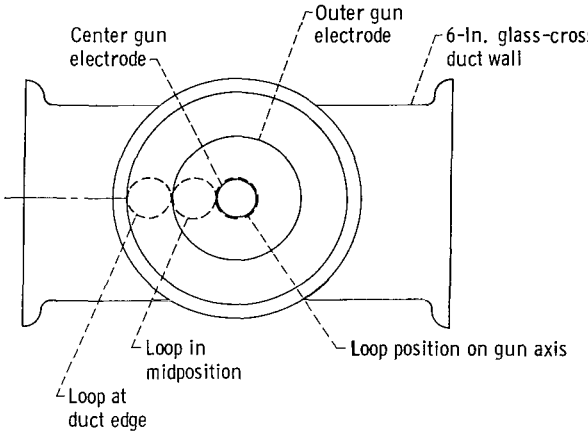

Figure 7. - Three positions of radial survey Rogovsky loop.

External loop. - Another measurement confirming this model is also the fact that the large external Rogovsky loop (enclosing this exhaust as well as the glass duct) shows no net axial currents in the duct anywhere near plasma currents in magnitude. The crude summing of unidirectional currents flowing in the later arriving exhaust agrees semiquantitatively with electrode current. The electrode current is shown for comparison in figure 6. The currents were summed for the various locations and area weighting was considered. This agreement, plus the frame views already described, shows connected currents of the order of the gun electrode current (in phase and synchronization with the gun electrode current) flowing in the exhaust plume. This phenomenon of axial currents flowing in the exhaust appears later than the extrapolated magnetic-front arrival time, but it is coincident with the arrival of the pinch-core front structure at the measuring station.

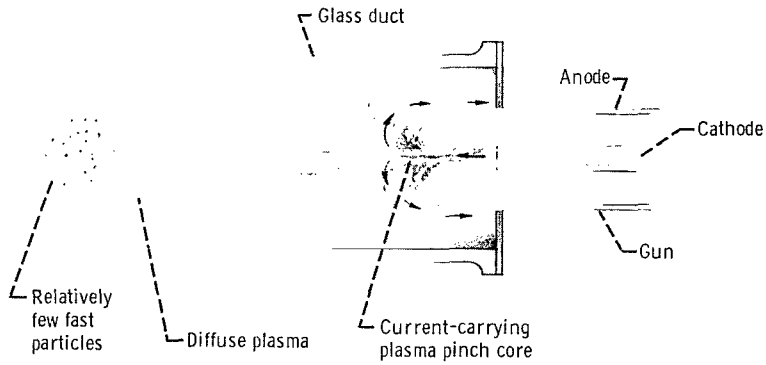

Figure 8. - Exhaust model. CD-7900

Exhaust Model

The combination of views and signals noted by loops provides verification of connected cylindrically symmetrical currents flowing axially in the later developing plasma structure. The central core of the current-carrying plasma "pinches" off the end of the center electrode, the "pinch" occuring under the action of the self-azimuthal magnetic-field pressure on the core. The exhaust takes on the following three separate characteristics:

(1) There are relatively few fast particles out in front.

(2) These are followed by a diffuse plasma (not carrying axial currents) predicted in position and velocity as if it were an extrapolation of the magnetic front noted in the gun annulus.

(3) This, then, is followed by a later developing, cylindrically symmetrical pinch-core structure (carrying gross axial currents still connected to the electrode). A time-resolved energy spectrum of the exhaust particles is needed to separate the relative contributions of each phenomenologically divided part of the exhaust plume before this mode can be compared with other gun modes. The influence of the surrounding duct must be kept in mind. This experiment has duct walls only 5 inches larger in diameter than the gun outer electrode diameter, so the wall perturbs the exhaust to some extent. This will not change the general structure of the exhaust but will influence details. The type of propellant used will also change the details.

IMPLICATIONS AFFECTING OTHER MEASUREMENTS

The complicated nature of the exhaust of the self-crowbar mode of operation coaxial plasma gun suggests caution in interpreting various measurements of gun performance utilizing exhaust measurements (even though most of the circuit energy has been dissipated before the current sheet exits the gun).

Since the pinch core portion of the exhaust is connected to and concentrated off the tip of the center electrode, erosion influence on the exhaust must be considered, and the energy spectrum of nonpropellant species will be needed. The presence of the pinch core forces more attention to the time-resolved knowledge of the ratio of directed energy to thermal energy of the exhaust. The fact that connected currents exist in the exhaust require caution in interpreting pendulum, calorimeter, and probe data. The high pinch core energy density is noted in the damage to calorimeter cups and can create erroneous impulse measurements due to cup material evaporation where the high-

energy-density core strikes the cup.

CONCLUSIONS

The results of Rogovsky loop, magnetic probe, and frame and streak photography of the exhaust of a self-crowbar mode of operation of a Marshall type coaxial plasma gun provide two general conclusions.

1. Three time-separated gross exhaust phases occur for each shot. Early exhaust is a relatively few fast particles and is noted only indirectly in this report. The next exhaust phenomenon in time (for the same shot) is a diffuse plasma, not carrying any axial currents, but having a velocity and time of arrival the same as if it were an extension of the magnetic front that existed earlier in the gun annulus. The last exhaust phenomenon in time is a later developing axially symmetric current structure that remains connected to the electrodes. It carries significant axial currents, has a pinch core center with core speed of slower velocity than the magnetic fronts in the gun annulus, and with time-varying decreasing velocity.

2. The fact that the third phase of the exhaust phenomenon carries gross axial and gun-connected currents suggests caution in exhaust diagnostics and measurement techniques.

Lewis Research Center
National Aeronautics and Space Administration
Cleveland, Ohio, October 1, 1964

REFERENCES

1. Marshall, John: Hydromagnetic Plasma Gun. Plasma Acceleration, S. W. Kash, ed., Stanford Univ. Press, 1960, pp. 60-72.

2. Michels, C. J., and Ramins, P.: Performance of Coaxial Plasma Gun with Various Propellants. Phys. of Fluids, pt. II, vol. 7, no. 11, Nov. 1964, pp. S71 to S74.

3. Lovberg, R. H., Hayworth, B. R., and Gooding, T. J.: The Use of a Coaxial Gun for Plasma Propulsion. Rep. AE62-0678, General Dynamics/Astronautics, May 15, 1962.

4. Gloersen, P., Gorowitz, B., and Palm, W.: Experimental Performance of a Pulsed Gas Entry Coaxial Plasma Accelerator. Rep. R61SD042, General Electric Co., Apr. 1961.

5. Kvartskhava, I. F., Meladze, R. D., and Suladze, K. V.: Experiments on Electrodynamic Acceleration of Plasmas. Soviet Phys. Tech. Phys., vol. 5, no. 3, Sept. 1960, pp. 266-273.

6. Burkhardt, L. C., and Lovberg, R. H.: Current Sheet in a Coaxial Plasma Gun. Phys. of Fluids, vol. 5, no. 3, Mar. 1962, pp. 341-347.

7. Hagerman, D. C., and Osher, J. E.: Two High Velocity Plasma Guns. Rev. Sci. Instr., vol. 34, no. 1, Jan. 1963, pp. 56-60.

8. Thom, Karlheinz, and Norwood, Joseph: Magnetic Ignition of Pulsed Gas Discharges in Air of Low Pressure in a Coaxial Plasma Gun. NASA TN D-910, 1961.

9. Starr, W. L., and Naff, J. T.: Acceleration of Metal Derived Plasma. Plasma Acceleration, S. W. Kash, ed., Stanford Univ. Press, 1960, pp. 47-59.

10. Dattner, A.: Acceleration of Plasma. Proc. Fourth Int. Conf. on Ionization Phenomena in Gases. N. R. Nilsson, ed., North-Holland Pub. Co., 1960, pp. IVE 1151-1155.

11. Patrick, Richard M.: The Production and Study of High Speed Shock Waves in a Magnetic Annular Shock Tube. Res. Rep. 59, Avco-Everett Res. Lab., Avco Corp., July 1959.

12. Keck, J. C., Fishman, F., and Petschek, H.: Current Distribution and Flow Model for Large Radius-Ratio MAST. Res. Rep. 117, Avco-Everett Res. Lab., Avco Corp., Jan. 1962.

13. Mawardi, O. K., and Naraghi, M. N.: Experimental Study of Current Sheets. Paper T3, Bull. Am. Phys. Soc., ser. II, vol. 8, no. 5, 1963, p. 440.

14. Mather, J.: Formation of a High-Density Deuterium-Plasma Focus in a Coaxial-Gun Device. Paper WI, Bull. Am. Phys. Soc., ser. II, vol. 9, no. 3, 1964, p. 339.

15. Marshall, J.: Performance of a Coaxial Plasma Gun. Paper Presented at Int. Symposium on Plasma Coaxial Guns, Case Inst. Tech., Cleveland (Ohio), Sept. 6, 1962.

16. Burkhardt, L. C., Knapp, E. A., and Williams, A. H.: Cathode Surface Effects on Axial Deuteron Acceleration and upon Neutron Production in a Coaxial Plasma Gun. Paper T5, Bull. Am. Phys. Soc., ser. II, vol. 8, no. 5, 1963, p. 441.

17. Gooding, Terence J., Hayworth, Bruce R., and Lovberg, Ralph H.: Development of a Coaxial Plasma Gun for Space Propulsion. GDA 63-0454, General Dynamics/Astronautics, May 15, 1963.

18. Lovberg, R.: Acceleration of Plasma by Displacement Currents Resulting from Ionization. Rep. GA-4363, General Atomic Div. General Dynamics Corp., June 1963.

19. Patrick, R. M., and Camac, M.: Experimental Investigation of Collision-Free Shocks and Plasma. Res. Rep. 122, Avco-Everett Res. Lab., Sept. 1961.

20. Lukyanov, S. Yu., Podgornyi, I. M., and Chuvatin, S. A.: Electrodynamic Acceleration of Plasmoids. III (Coaxial System.) Soviet Phys. Tech. Phys., vol. 6, no. 9, Mar. 1962, pp. 750-754.

21. Gorowitz, B., Gloersen, P., and Rowe, J. H.: Performance Study of a Repetitively Pulsed Two-Stage Plasma Propulsion Engine. Space Sci. Lab., General Electric Co., Nov. 20, 1963.

22. Lovberg, R. H.: Measurement of Plasma Density in a Rail Accelerator by Means of Schlieren Photography. Rep. GA-4735, General Atomic Div., General Dynamics Corp., Nov. 1963.

23. Eubank, H. P., and Wilkerson, T. D.: Ion Energy Analyzer for Plasma Measurements. Rev. Sci. Instr., vol. 34, no. I, Jan. 1963, pp. 12-18.

24. Ashby, D. E. T. F.: The Flow of High Energy Plasma in a Magnetic Guide Field. Paper Presented at Sixth Int. Conf. on Ionization Phenomena in Gases, Paris (France), July 1963.

25. Eubank, Harold P.: Impurity Content of Plasma Produced by a Coaxial Plasma Gun. Phys. of Fluids, vol. 6, no. 10, Oct. 1963, pp. 1522-1524.

26. Ashby, D. E. T. F.: The Entry of a Tenuous Plasma Into an Axial-Magnetic Field. Paper Q7, Bull. Am. Phys. Soc., ser. II, vol. 9, no. 3, 1964, p. 331.

27. Glasstone, Samuel, and Lovberg, Ralph H.: Controlled Thermonuclear Reactions. D. Van Nostrand Co., 1960, p. 165.

28. Rose, David J., and Clark, Melville, Jr.: Plasmas and Controlled Fusion. M.I.T. Press/John Wiley & Sons, Inc., 1961, p. 360.

"The aeronautical and space activities of the United States shall be conducted so as to contribute . . . to the expansion of human knowledge of phenomena in the atmosphere and space. The Administration shall provide for the widest practicable and appropriate dissemination of information concerning its activities and the results thereof."

—NATIONAL AERONAUTICS AND SPACE ACT OF 1958

NASA SCIENTIFIC AND TECHNICAL PUBLICATIONS

TECHNICAL REPORTS: Scientific and technical information considered important, complete, and a lasting contribution to existing knowledge.

TECHNICAL NOTES: Information less broad in scope but nevertheless of importance as a contribution to existing knowledge.

TECHNICAL MEMORANDUMS: Information receiving limited distribution because of preliminary data, security classification, or other reasons.

CONTRACTOR REPORTS: Technical information generated in connection with a NASA contract or grant and released under NASA auspices.

TECHNICAL TRANSLATIONS: Information published in a foreign language considered to merit NASA distribution in English.

TECHNICAL REPRINTS: Information derived from NASA activities and initially published in the form of journal articles.

SPECIAL PUBLICATIONS: Information derived from or of value to NASA activities but not necessarily reporting the results of individual NASA-programmed scientific efforts. Publications include conference proceedings, monographs, data compilations, handbooks, sourcebooks, and special bibliographies.

Details on the availability of these publications may be obtained from:

SCIENTIFIC AND TECHNICAL INFORMATION DIVISION

NATIONAL AERONAUTICS AND SPACE ADMINISTRATION

Washington, D.C. 20546